Journal for Electrochemistry and Plating Technology

JEPT

Edited by: DGO-Fachausschuss Forschung – Hilden / Germany

Investigation of nucleation mechanism and surface morphology of the crystallites in zinc-cobalt alloy coating

In present investigation, a new brightener was synthesized by condensation of 3, 4, 5-Trimethoxy benzaldehyde and Glycine (TG). Hull cell experiments were conducted to optimize the plating bath components and operating parameters. To examine the influence of TG on nucleation mechanism of Zn-Co alloy electrodeposition, cyclic voltammetry and chronoamperometry study was carried out. Schariffker and Hills model was used to analyze current transients, which in presence of TG confirmed instantaneous nucleation. Corrosion studies were done using potentiodynamic polarization and electrochemical impedance spectroscopic technique, in 3.5 wt. % NaCl for bright and dull ...

Received: 2020-12-24
Received in revised form: 2021-03-15
Accepted: 2021-03-18

Keywords: Zinc-cobalt alloy crystallites, Nucleation; Brightener, codeposition

Authors:
Jyoti S. Kavirajwar and S. Basavanna

DOI: 10.12850/ISSN2196-0267.JEPT7151

LEUZE VERLAG
seit 1902

Investigation of nucleation mechanism and surface morphology of the crystallites in zinc-cobalt alloy coating

Jyoti S. Kavirajwar[1] and S. Basavanna[2]

1) Department of Chemistry, APS College of Arts and Science, Bangalore, Karnataka, INDIA

2) Department of Chemistry, Prerana PU College, Tumkur-572103, Karnataka, INDIA

In present investigation, a new brightener was synthesized by condensation of 3, 4, 5-Trimethoxy benzaldehyde and Glycine (TG). Hull cell experiments were conducted to optimize the plating bath components and operating parameters. To examine the influence of TG on nucleation mechanism of Zn-Co alloy electrodeposition, cyclic voltammetry and chronoamperometry study was carried out. Schariffker and Hills model was used to analyze current transients, which in presence of TG confirmed instantaneous nucleation. Corrosion studies were done using potentiodynamic polarization and electrochemical impedance spectroscopic technique, in 3.5 wt. % NaCl for bright and dull zinc-cobalt alloy coatings. Phase structure, surface morphology and brightness of the deposit were characterized by X-ray diffraction analysis, scanning electron microscopy and reflectance studies. These studies revealed the role of TG in modifying the nucleation mechanism and surface morphology of zinc-cobalt alloy crystallites and thereby producing a bright corrosion resistant Zn-Co alloy coating on mild steel substrate.

Keywords: Zinc-cobalt alloy crystallites, Nucleation; Brightener, codeposition
Paper: Received: 2020-12-24 / Received in revised form: 2021-03-15 / Accepted: 2021-03-18
DOI: 10.12850/ISSN2196-0267.JEPT7151

1 Introduction

The electrodeposition of zinc-cobalt alloys has drawn a lot of attention because these alloys show significantly increased corrosion resistance than pure zinc [1]. The alloying elements successfully used with zinc are iron, cobalt and nickel. The fundamental function of iron, cobalt and nickel along with zinc is to modify the corrosion potential of deposit. The alloy becomes slightly nobler than zinc and hence the corrosion rate of the alloy is slowed. At the same time, the deposit is still sacrificial with respect to steel. Consequently the same thickness of an alloy has the ability to protect the underlying steel for a longer time than conventional zinc [2]. Coating with low cobalt content are less noble than steel so that they represent a sacrificial type of coating. Those with increased cobalt content are nobler than steel and provide barrier type of protection [3]. Only about 1 wt. % of cobalt is needed when alloying zinc with cobalt to obtain similar corrosion resistance to zinc-nickel (10–14 wt. %).

As characterized by Brenner et al., the electrodeposition of Zn-Co alloys from aqueous plating baths is the anomalous type of codeposition; that is, the less noble component, zinc, deposits preferably with respect to the more noble cobalt. Because of this fact, the cobalt content in the zinc-cobalt alloys produced from aqueous plating

baths is usually low. The electrodeposition of Zn–Co alloys with a controlled morphology and composition has been investigated as a result of their improved corrosion resistance.

From the available literature it is well known that additives which are often organic compounds yield coatings with desirable surface properties. Organic compounds containing oxygen, sulphur and nitrogen are amongst the most widely used additives in modern electroplating. These compounds can adsorb on the growing deposits or on the substrate with an impact on deposit properties and the electroplating process [4].

Zinc and its alloy coatings, in presence of additive called 'Brightener' further increase corrosion resistance ability and help to improve the surface morphology of the coating [5–7]. Hence presently there is more focus on these studies. Though enough literature is available on zinc-cobalt alloy coatings in presence of various brighteners but much information on the mechanism of zinc-cobalt alloy co-deposition and mode of nucleation mechanism is not mentioned. Hence in the present work, an attempt has been made to investigate the codeposition mechanism and mode of nucleation, with attention also being given to deposit morphology and composition.

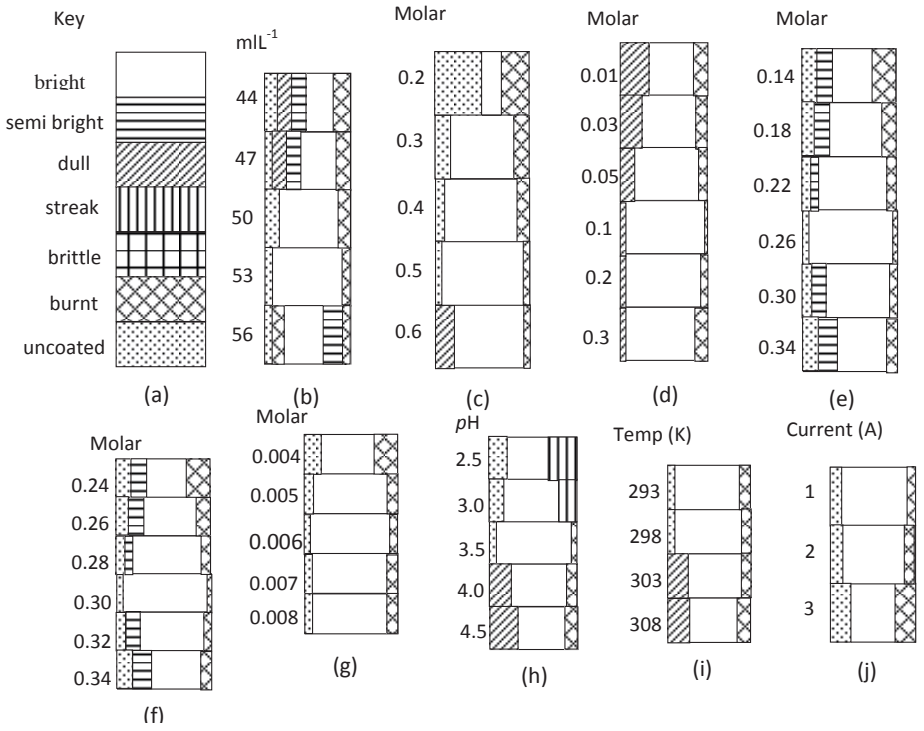

Fig. 1: Hull cell experimental results: (a) Key, Influence of (b) Brightener (TG) (c) Zinc Sulphate (d) Cobalt Chloride (e) Sodium sulphate (f) Boric acid (g) Cetyl trimethyl ammonium bromide (CTAB) (h) pH (i) Temperature (j) Current

Voltammetry was used to study the codeposition mechanism. Chronoamperometry was used to explain the nucleation mode and techniques such as SEM and XRD were used to characterize the deposits obtained under different conditions.

2 Experimental

2.1 Preparation of brightener

Condensation product of 3, 4, 5-Trimethoxy benzaldehyde and Glycine (TG) was selected as a brightener to obtain bright coatings. Condensation product was synthesized by using analytical grade chemicals. Equimolar concentration of Glycine and 3, 4, 5-Trimethoxy benzaldehyde were mixed and condensed in 50 ml acetic acid medium, in a reflux condenser. A magnetic stirrer was used for stirring the mixture and heating was done on a hot plate for approximately 3 hrs, at 343K temperature [8].

Thin layer chromatography technique was used to confirm the formation of condensation product. Dilution of this condensation product obtained was done with distilled water, in a 100 ml standard flask. A fixed volume of this newly synthesized organic additive solution (TG) was included in a zinc-cobalt basic bath solution and stirred for 45 minutes using magnetic stirrer, before carrying out the Hull cell experiments.

2.2 Preparation of optimized zinc-cobalt plating bath and electrodeposition process

Electrodeposition was done using miniature plating tank called 'Hull cell'. Condensation product TG was added in plating bath solution and its optimized concentration (53 ml) was determined using the Hull cell experiment. Optimization of every other component present in the bath and its operating parameters was done by repeating the Hull cell experiments in the range depicted in Hull cell codes (*Fig. 1*). *Table 1* gives the optimized composition of zinc-cobalt plating bath solution.

2.3 Electrodeposition process

Pretreatment was given to the steel plate by using organic solvent, emery paper, rinsed with distilled water and dried. Pure zinc plate acted as anode and the cathodic material was a pretreated mild steel plate. Using a Hull cell, DC power supply, anode and cathode, electrodeposition was done for 10 minutes.

Plated Hull cell panels (mild steel plates coated in absence and presence of brightener) were used for corrosion, electrochemical and surface morphological studies.

Corrosion studies were done by Electrochemical Impedance Spectroscopy and Polarization

Tab. 1: Composition of optimized zinc-cobalt bath and its operating conditions

Bath components	Concentration	Operating Conditions
$ZnSO_4$	0.5 M	Anode: Zinc plate (99.9 %)
$CoCl_2.6H_2O$	0.1 M	Cathode: Mild steel plate
$NaSO_4$	0.26M	pH: 3.5
H_3BO_3	0.3 M	Temperature: 293–303 K
CTAB	0.006 M	Plating time: 10 min
Brightener (TG)	53 mlL^{-1}	Bright Current density range: 3.0–6.5Adm^{-2}

techniques using electrochemical workstation (Model: CHI660D). Zinc-cobalt coated steel plate acted as working electrode, platinum foil as counter electrode and SCE as reference electrode. Scan rate was 0.05 V/s in the range of potential -0.1 V to -1.4 V. Frequency range for EIS was in between 100 KHz and 1 Hz with perturbation signal amplitude of 0.005 V. Surface morphological studies were done using SEM, XRD and reflectance spectroscopy. Texture coefficient is calculated using the formula given in the earlier literature [27]. Standard JCPDS powder diffraction file card (JCPDS Zn-Co 29-0523) was used to obtain data for finding texture coefficient. Percentage reflectance was measured using USB 4000 reflectance spectrophotometer [27].

3 Results and Discussion

3.1 Cyclic voltammetry studies

Electrochemical behavior of zinc-cobalt alloy deposit on mild steel was studied using cyclic voltammetry technique. During cathodic scan in dull deposit, cathodic peak potential was noted at -1.264V (E_1). It is related with simultaneous discharge of both Zn^{2+} ion and Co^{2+} ion to zinc atom and cobalt atom. When the sweep direction is reversed, two crossovers are seen in cathodic region of voltammogram. Nucleation over potential is the first crossover potential, which occurs at more cathodic region and is denoted by symbol E_η [9, 10]. Second crossover potential at zero current region occurs at potential of -1.148 V and is denoted by symbol E_{co}. These crossovers form distinguishing attributes of three Dimensional crystal growth processes. In dull coat, four peaks of oxidation (A_1, A_2, A_3 and A_4) also called anodic peaks are seen in the voltammogram. Numerous anodic peaks are detected during oxidation of zinc-cobalt alloy, due to formation of various intermediate phases of zinc and zinc-cobalt alloy in deposit. Multiple anodic peaks indicate the presence of multiple phases in zinc-cobalt alloy deposit. These 4 phases are η-phase of zinc, γ-phase of zinc, η-phase of cobalt and γ-phase of cobalt [11]. Anodic peak observed at -0.889 V (A_1) indicates zinc oxidation from η-phase which is unadulterated phase of zinc and that observed at -0.603 V (A_2) indicates the oxidation of zinc from γ-phase. Anodic peaks at -0.478 V (A_3) and -0.261 V (A_4) indicate cobalt oxidation from η-phase and zinc oxidation from γ-phase respectively [11].

In bright deposit, cathodic peak potential (E_2) was noticed at -1.298 V, higher negative potential, indicating adsorption of TG on the cathode

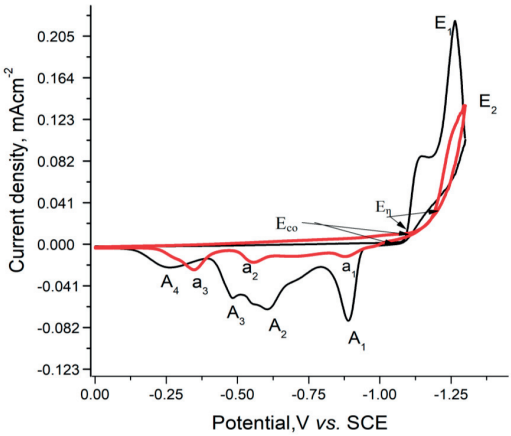

Fig. 2: Typical cyclic voltammogram of zinc-cobalt alloy coating obtained from optimized zinc-cobalt bath solution, 0.5 M $ZnSO_4$ + 0.1 M $CoCl_2$ + 0.26 M Na_2SO_4 + 0.3 M H_3BO_3 + 0.006 M CTAB, pH = 3.5 in bright and dull zinc-cobalt alloy deposit, at scan rate of 0.05 Vs^{-1} and in the potential range of -0.1 V to -1.4 V (Red colored line indicates bright Zn-Co alloy deposit and black colored line indicates dull Zn-Co alloy deposit)

thereby leading to obstruction near electrode surface and hence inhibiting discharge of zinc and cobalt ions, finally resulting in decrease of grain size [9]. This has been confirmed with SEM and X-Ray diffraction studies. Voltammogram shows three broad anodic peaks (A_1, A_2 and A_3) at -0.881 V, -0.557 V and -0.348 V. First broad peak (a_1) indicates zinc oxidation from η-phase, second peak (A_2) indicates Zinc oxidation from γ-phase and third peak (A_3) indicates cobalt oxidation from η-phase and γ-phase.

It was found that in presence of TG, anodic peaks are a bit shifted towards positive potential. It's a clear indication of the fact that, presence of TG in plating bath makes oxidation of zinc and cobalt more difficult, resulting in reduction of the grain size of zinc-cobalt alloy crystallites thereby making it appear more smooth, compact and uniform [12]. In bright deposit the cathodic peak potential was observed at -1.298 V. Most probably, TG adsorbs on cathodic surface. Hence there is shift in cathodic peak potential towards more negative direction. When this phenomenon happen a portion of surface area is blocked by TG [11]. Consequently, zinc and cobalt ions get reduced at remaining portion of the surface area that was not blocked. When overvoltage is increased then TG gets desorbed allowing reduction of zinc and cobalt ions at the blocked area. On reversing the potential scan in opposite direction, four anodic peaks with decreasing peak height are noticed, corresponding to zinc and cobalt oxidation from η- and γ-phases [11].

Tab. 2: Experimental data noted from voltammogram (η is overvoltage, E_{co} is Crossover potential and E_c is cathodic peak potential)

Type of coating	Ec / V	Eco / V	η / V
Dull coat	-1.264	-1.098	0.166
Bright coat	-1.298	-1.116	0.182

This result indicates that due to partial adsorption of TG on cathode, dissolution process is hindered. Hence it confirms the formation of more compact bright zinc-cobalt alloy coating.

3.2 Current transient examination

Current transients were examined under given experimental conditions, to explore the nucleation mechanism involved in dull and bright zinc-cobalt alloy coating on steel. Most important factor accountable for the creation of refined deposit is production of new nucleation sites and growth rate of crystallites. Electrocrystallisation is a process of new phase formation and chronoamperometry is an effective technique to explain this process [12].

Figure 3 depicts current-time transients noted in reduction of zinc and cobalt ion, in potential range from –1.20 V to -1.28 V, in case of dull and bright zinc-cobalt alloy coating. The transient behavior is characteristic of nucleation mechanism, exhibiting three dimensional (3D) nuclei expansion.

Nucleation process was illustrated using 3D nucleation models, whose equations for instantaneous and progressive mode are given as below:

Instantaneous mode

$$\left(\frac{I}{I_{max}}\right)^2 = \frac{1.9542}{t/t_{max}}\left\{1-\exp\left[-1.2564\left(\frac{t}{t_{max}}\right)\right]\right\}^2$$

Progressive mode

$$\left(\frac{I}{I_{max}}\right)^2 = \frac{1.2254}{t/t_{max}}\left\{1-\exp\left[-2.3367\left(\frac{t}{t_{max}}\right)^2\right]\right\}^2$$

Non-dimensional plots obtained from theoretical as well as experimental data of dull and bright zinc-cobalt alloy coatings are depicted in *Figure 4* at different potentials.

According to the conventional theorem, electrochemical reduction of iron-group metal ions on the cathode surface follows the mechanism given below [13].

$$2H_2O + 2e^- \rightarrow H_2 + 2OH^- \quad <3>$$

$$M^{2+} + OH^- \rightarrow M(OH)^+ \quad <4>$$

$$M(OH)^+ \rightarrow M(OH)_{ads}^+ \quad <5>$$

$$M(OH)_{ads}^+ + 2e^- \rightarrow M + OH^- \quad <6>$$

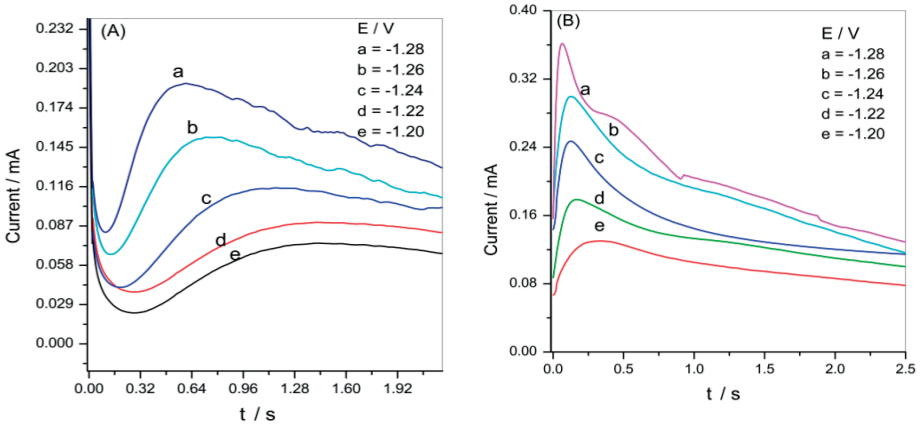

Fig. 3: Current transients for zinc-cobalt electrodeposition from 0.5 M $ZnSO_4$ + 0.1 M $CoCl_2$ + 0.26 M Na_2SO_4 + 0.3 M H_3BO_3 + 0.006 M CTAB, pH: 3.5, Current density: 3.5 Adm^{-2} in (A) dull (B) bright zinc-cobalt alloy coating

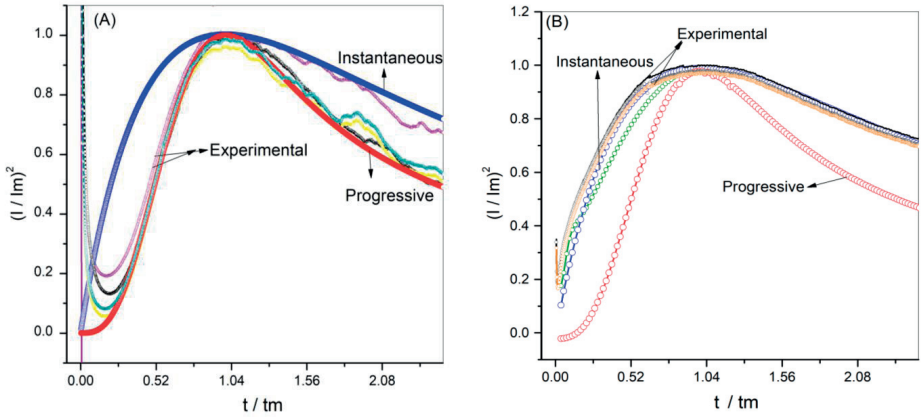

Fig. 4: Non-dimensional $(I/I_{max})^2$ vs. t/t_{max} plot for zinc-cobalt alloy electrodeposition obtained from 0.5 M $ZnSO_4$ + 0.1 M $CoCl_2$ + 0.26 M Na_2SO_4 + 0.3 M H_3BO_3 + 0.006 M CTAB, pH = 3.5, Current density = 3.5 Adm^{-2} in (A) dull (B) bright zinc-cobalt alloy coating

Where M designates iron, cobalt, and nickel metal. Reduction rate of M mainly depends on the stability of $M(OH)_{ads}^{+}$ or $M(OH)^{+}$. Stability of zinc and cobalt metal monohydroxide ions is in the following order: $Co(OH)^{+} > Zn(OH)^{+}$ hence the content of cobalt in coating is much lower than that of zinc.

Meanwhile the nucleation or growth process of Zn-Co deposit is always coupled with release of hydrogen gas, which is evident from the equation <3> and <6>. Hence the experimental $(I/I_m)^2$ is always greater than theoretical $(I/I_m)^2$.

Nucleation mechanism of dull zinc-cobalt alloy coat is depicted in *Figure 4 (A)*. The growing part of transients is positioned on theoretical progressive curve.

Nucleation mechanism of bright zinc-cobalt alloy coat is depicted in *Figure 4 (B)*. The current transients are located on instantaneous nucleation curve. This result proved that in case of bright zinc-cobalt alloy deposit the nucleation process occurs by instantaneous mode.

An additional analytical aspect depends on the growing part of transient curves, based on early stage deposition study [12, 14]. It is possible to plot I versus $t^{1/2}$ denoting instantaneous nucleation and I versus $t^{3/2}$ denoting progressive nucleation.

Figure 5 (A) shows plot of I versus $t^{3/2}$ observed for dull zinc-cobalt alloy deposit under the given experimental conditions and confirms progressive nucleation mechanism.

Figure 5 (B) shows plot of I versus $t^{1/2}$ observed for bright zinc-cobalt alloy deposit under the same experimental conditions and confirms instantaneous nucleation mechanism [15–18].

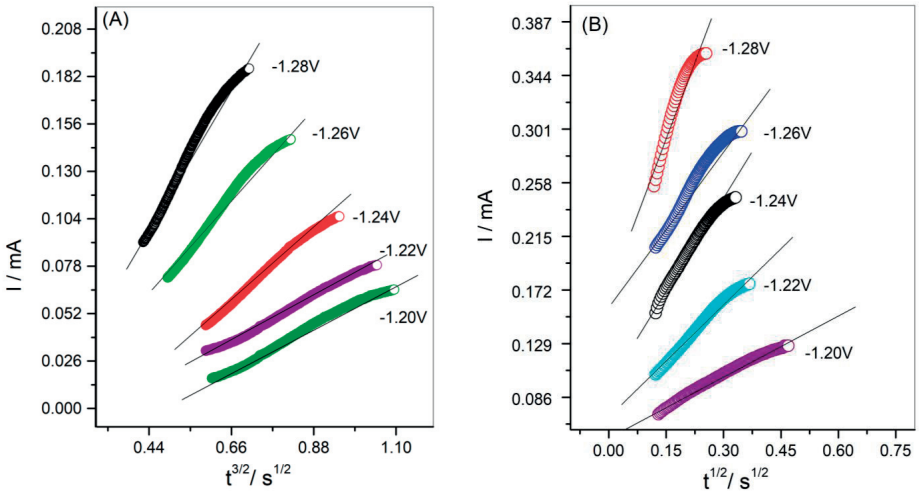

Fig. 5: (A) Dependence between I versus $t^{3/2}$ plot for preliminary transient portion of dull zinc-cobalt alloy electrodeposit (from *Fig. 3 (A)*), and *(B)* Dependence between I versus $t^{1/2}$ plot for preliminary transient portion of bright zinc-cobalt alloy electrodeposit (from *Fig. 3 (B)*)

3.3 Impedance and polarization studies

Electrochemical impedance spectroscopy and Tafel polarization technique was used for determining the corrosion resistance and hence, the protection ability of dull and bright zinc-cobalt alloy coating.

Figure 6 (A) shows Nyquist impedance plot of zinc-cobalt alloy deposits in absence and presence of TG. Charge transfer resistance value of dull and bright deposit was found to be 170 Ωcm^2 and 1359 Ωcm^2 respectively. This result reveals that bright zinc-cobalt alloy coating enhances corrosion resistance ability thereby diminishing the corrosion rate of steel. The simulation program was used to build the proposed equivalent circuit and fit it to the experimental data (Inset *Fig. 6 (A)*). This was done to explain the corrosion behavior of zinc-cobalt alloy coatings [18, 19].

Figure 6 (B) shows the Tafel curves where the I_{corr} value is found to be 1.136 mA/cm^2 for dull deposit and 0.0254 mA/cm^2 for bright deposit. There is decrease in I_{corr} value. E_{corr} value of dull and bright deposit is -0.9997 V and -0.9499 V respectively. The E_{corr} value shifts in more noble direction, indicating an increase in corrosion resistance. This result infers that the bright zinc-cobalt alloy electrodeposit is successful in acting a good coating for protection of mild steel [18–23].

3.4 Operating window of plating bath

Throwing power and current efficiency are important factors in determining the efficiency of the plating bath. Optimized zinc-cobalt bath solution was taken in a specially designed methacrylate container called Haring Blum cell to measure its current efficiency and throwing power.

Experimental results obtained are depicted in *Table 3* and *Figure 7*. Experimental data shows 4 A/dm^2 as the optimized current density for the zinc-cobalt plating bath. It also confirms that current density (current per unit area) is an impor-

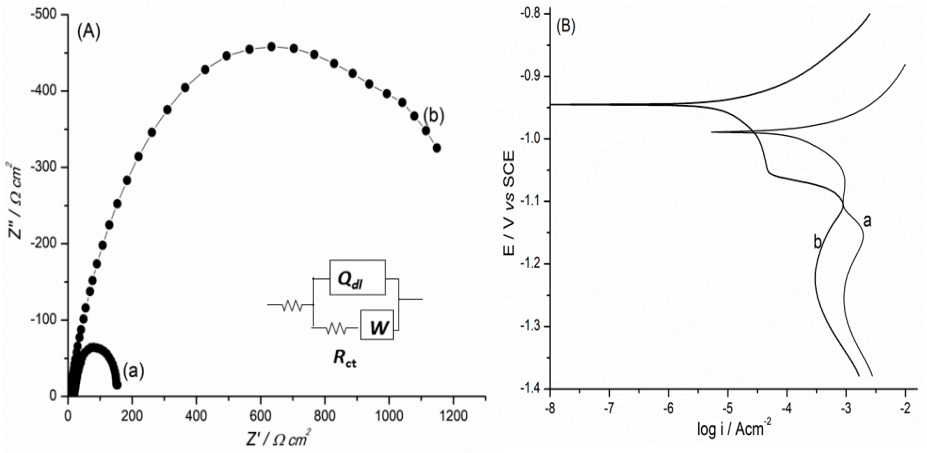

Fig. 6: (A) Nyquist impedance plot, (B) Tafel polarization curves of (a) dull (b) bright Zn-Co alloy coating obtained in 3.5 weight % sodium chloride solution

tant parameter in determining the current efficiency and throwing power of plating bath, which in turn determines the quality of plating bath.

3.5 Adhesion and porosity measurements

Adhesion was detected using 'Bend test'. Coated steel plates were bent to 180°. Even after 180° bending, no crack or peel off in coating was noticed. This showed improvement in adherence of zinc-cobalt alloy coating.

Porosity measurement was done using Ferroxyl test. Number of blue spots per unit area of dull and bright deposit was counted. In case of bright deposit the blue spots were comparatively less which indicated that it was comparatively less porous or in other words more compact.

Tab. 3: Throwing power and current efficiency at dissimilar current densities

Current density (Adm-2)	Current efficiency (%)	Throwing power (%)
1	20	65
2	21	68
3	24	70
4	30	76
5	25	70
6	20	20

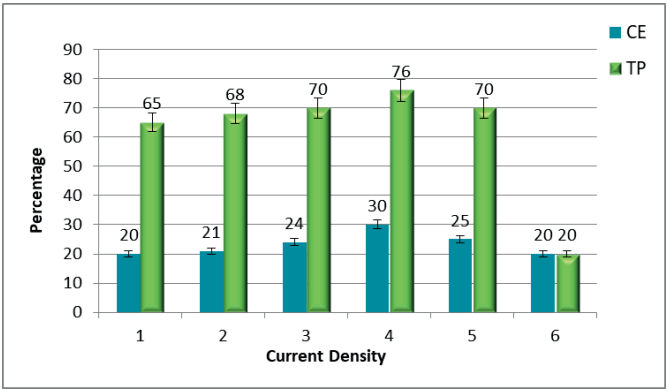

Fig. 7: Comparison of throwing power and current efficiency of optimized zinc-cobalt bath solution at different current densities

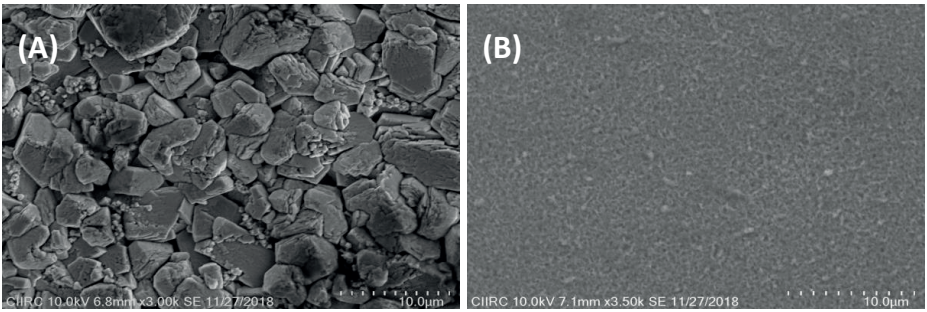

Fig. 8: Scanning electron microscopic images of zinc-cobalt alloy deposit in (A) dull and (B) bright zinc-cobalt alloy coating

3.6 Analysis of surface morphology by scanning electron microscopy and reflectance spectroscopy

Scanning electron microscopic images (*Fig. 8 (A)*) depict irregular and coarse-grained zinc-cobalt alloy deposit, in absence of TG. When TG is added in plating bath it enhances the formation of new nuclei during electrodeposition progression, simultaneously decreasing enlargement of zinc-cobalt alloy nuclei, resulting in the formation of refined deposit of zinc-cobalt crystallites (*Fig. 8 (B)*). This results in the formation of smooth and bright coating [18, 19, 22].

Figure 9 depicts the reflectance and degree of reflection in dull and bright zinc-cobalt coating. It is clearly visible from the reflectance spectra that the inclusion of TG into the plating bath results in enhancement of reflection. Only 4–5 % of difference in reflectance was noticed at different points on the surface of zinc-cobalt alloy coatings [11]. These results confirmed that TG can be used as a superior brightening agent for zinc-cobalt alloy coatings [11, 24].

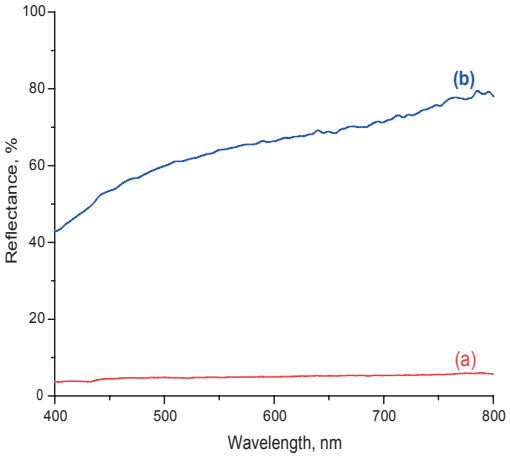

Fig. 9: Reflectance spectra of zinc-cobalt alloy electrodeposition at 3.5 Adm^{-2} in (a) dull (b) bright zinc-cobalt alloy coating

3.7 X-Ray diffraction study

This method of analysis was utilized to know various parameters such as phases present in the zinc-cobalt alloy coatings, size of crystallites and the preferred orientation of crystallites in dull and bright zinc-cobalt alloy coating. In brief, we can say that the influence of TG on structure of the zinc-cobalt alloy deposit was investigated.

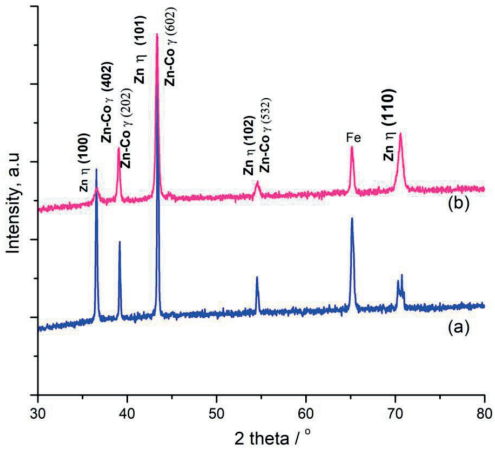

Fig. 10: X-Ray diffraction pattern of zinc-cobalt alloy electrodeposition observed in (a) dull and (b) bright zinc-cobalt alloy deposit

Figure 10 shows the XRD spectra for dull and bright zinc-cobalt alloy coating. X-Ray diffraction spectra show the presence of η- and γ-phase of zinc (*Fig. 10*). In the XRD spectra, few peaks con-

firm the presence of η-phase of pure zinc metal while some of them confirm the presence of γ-phase of zinc-cobalt alloy [25]. Also, it does not show peaks of any other elements indicating that there are no impurities in the deposit. Phase modification could be reflected by dissimilar appearance of the dull and bright coating in the SEM images.

Diffraction pattern also shows the broadening of X-ray diffraction peaks in bright zinc-cobalt alloy deposit. Broadening of XRD peaks usually correspond to reduction in the size of zinc-cobalt alloy crystallites in deposit which is also supported by SEM result, which confirmed the fine-grained nature of bright zinc-cobalt alloy deposit.

Figure 10 (a) and the texture coefficient calculations (*Fig. 11*), indicate (602) and (402) as the preferred orientations for zinc-cobalt alloy crystallites in the dull deposit. XRD spectrum of bright zinc-cobalt coating was different and is shown in *Figure 10 (b)*.

Figure 10 (b) and the texture coefficient calculations (*Fig. 11*), indicate (602) as the preferred orientations for zinc-cobalt alloy crystallites in bright deposit. Orientation in preferred direction arises because different faces of the crystal show different growth rates, which is due to adsorption of TG on cathode surface [26, 27]. To summarize, surface modifications like preferred orientation along (602) plane and refinement in grain structure of the zinc-cobalt alloy crystallites may be responsible for bright appearance of the coating.

4 Conclusions

1. The newly synthesized brightener (TG) in optimized zinc-cobalt bath produces 80 % reflectance resulting in a bright electrodeposit in the range of current density 3 A/dm^2 to 6.5 A/dm^2

2. Cyclicvoltammetric studies revealed multiple anodic peaks due to presence of η- and γ-phases of zinc-cobalt alloy in the deposits. This is also supported by X-Ray Diffraction spectra.

3. Chronoamperometry helped to categorize the three dimensional nucleation mechanisms in dull and bright zinc-cobalt alloy coating. It confirmed that in bright deposit, three-dimensional nucleation mechanism occurs by instantaneous mode.

4. Corrosion studies confirm increase in corrosion resistance of bright deposit, which is closely associated with decrease in grain size of zinc-cobalt alloy crystallites in deposit, supported by SEM and XRD investigations.

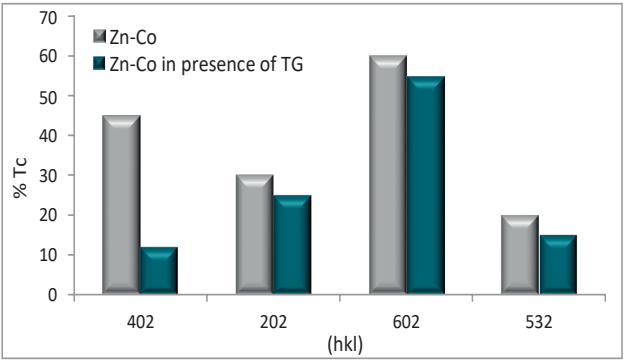

Fig. 11: Preferred orientation of dull and bright zinc-cobalt alloy deposit

5. Surface morphological studies were done by scanning electron microscopy and reflectance spectroscopy. SEM analysis of the coating showed formation of small clusters in bright deposit, promoting the formation of smooth and compact coatings. Reflectance spectra revealed increase in percentage reflectance of bright Zn-Co alloy coating.

6. XRD spectra revealed broadening of the peaks in bright deposit indicating grain refinement. Presence of gamma phase of zinc-cobalt alloy in the coating attributed to increased corrosion resistance.

The proposed studies indicate that TG can be conveniently used as an efficient brightener and corrosion resistance enhancer, for zinc-cobalt alloy coatings on mild steel components, in various electroplating industries.

Acknowledgment

The authors are grateful to the Department of Chemistry, Kuvempu University for providing facilities to carry out this research.

References

[1] J.B. Bajat; S. Stankovic; B.M. Jokie: Electrochemical deposition and corrosion stability of Zn-Co alloys, J. Solid state electrochem, v. 13, (2009) 755–762

[2] M.S. Chandrasekar; S. Srinivasan; M. Pushpavanam: Properties of Zn alloy electrodeposits produced from acid and alkaline leectrolytes, J. Solid State Electrochem, v. 13, (2009) 781–789

[3] M. Mouanga; L.Ricq; P. Bercot: Electrodeposition and Characterization of zinc-cobalt alloy from chloride bath; influence of coumarin as additive, Surface and coatings Technology, v. 202, (2008) 1645–1651

[4] M. Mouanga; L.Ricq; P. Bercot: Effects of thiourea and urea on zinc-cobalt electrodeposition under continuous current, J. Applied Electrochem, v. 38, (2008) 231–238

[5] V. Narasimhamurthy, Ph.D. Thesis, Bangalore University, India (1996)

[6] E.R. Frischauf, E.W. Eckles, U.S. Patent. 40208(2000)

[7] X. Zhou; H. Li; Huafeng, L. Liu; B. Cailiao v. 32, (1999) 1

[8] D. Chen; A.E. Martell: Inorg. Chem. v. 26, (1987) 1026–1030

[9] K.O. Nayana; T.V. Venkatesha: Effect of ethyl vanillin on Zn-Ni alloy electrodeposition and its properties, Bull Material Sci., v. 37, (2014) 1137–1146

[10] Z. Zhang: Trans. Non-ferr Met Soc. China, v. 11(4), (2001) 603

[11] S. Basavanna; Y. Arthoba Nayaka: Electrochemical and reflectance studies of bright Zn-Co alloy coatings, Indian Journal of Chemical Technology, v. 19, (2012) 91–95

[12] B.R., Schariffker; G. Hills: Theoretical and experimental studies of multiple nucleation, Electrochimica Acta, v. 28, (1983) 879–889

[13] P. Tsay; C.C. Hu: Non-anomalous co-deposition of iron-nickel alloys using pulse reverse electroplating through means of experimental strategies, J. Electrochemical Society, v. 149, No.10, (2002) C492–C497

[14] Y. Liao; D.R. Gabe; G.D. Wilcox: A study of zinc-iron alloy electrodeposition using a rotating cylinder hull cell, Plat Surf Finish, v. 85, (1998) 60–66

[15] H.X. Zhang; C. Zhu; Q. Lu; H. Cai; Y.W. Luye: Electrodeposition of Nanocrystalline Ni–Fe Alloy Coatings Based on 1-Butyl-3-Methylimidazolium-Hydrogen Sulfate Ionic Liquid, Journal of nanoscience and Nanotechnology, v. 17, No. 2, (2017) 1108–1115; https://doi.org/10.1166/jnn.2017.12719

[16] S. Ghaziof; P.A. Kilmartin; W. Gao: Electrochemical studies of sol-enhanced Zn-Ni-Al2O3 composite and Zn-Ni alloy coatings, Journal of Electroanalytical chemistry, v. 755, (2015) 63–70; https://doi.org/10.1016/j.jelechem.2015.07.041

[17] H.F. Alesary; S. Cihangir; A.D. Ballantyne; R.C. Harris; D.P. Weston; A.P. Abbott; K.S. Ryder: Influence of Additives on the Electrodeposition of Zinc from a Deep Eutectic Solvent, Electrochemica acta, v. 304, (2019) 118–130

[18] Z. Feng; Q. Li; J. Zhang; P. Yang; M. An: Electrochemical Behaviours and Properties of Zn-Ni Alloys Obtained from Alkaline Non-Cyanide Bath Using 5, 5 -Dimethylhydantoin as Complexing Agent, Journal of The Electrochemical Society, v. 162, No. 9, (2015) D412–D422

[19] D.H. Abdeen; M. El Hachach; M. Koc; M.A. Atieh: A Review on the Corrosion Behaviour of Nanocoatings on Metallic Substrates, Materials, v.12, (2019) 210; doi:10.3390/ma12020210

[20] C. Oulmas; S. Mameri; D. Boughrara; A. Kadri; J. Delhalle; Z. Mekhalif; B. Benefedda: Comparative study of Cu-Zn coatings electrodeposited from sulphate and chloride baths, Heliyon, v. 5, (2019) 7, E02058; doi: 10.1016/j.heliyon.2019.e02058. e Collection 2019 Jul

[21] S. Anwar; F. Khan; Y. Zhang: Corrosion behaviour of Zn-Ni alloy and Zn-Ni nano-TiO2 composite coatings electrodeposited from ammonium citrate baths, v.141, (2020) 366–379

[22] O. Sanni; A.P.I. Popoola; O.S.I Fayomi: Enhanced corrosion resistance of stainless steel type 316 in sulphuric acid solution using eco-friendly waste product, Results in physics, v. 9, (2018) 225–230

[23] C. Lihong; C. Liu; D. Han; S. Ma; W. Guo; H. Cai; X. Wang: Effect of graphene on corrosion resistance of waterborne inorganic zinc-rich coatings, Journal of alloys and compounds, v. 774, (2019) 255–264

[24] S. Basavanna; Y. Arthoba Nayaka: Study of the effect of new brightener on Zn-Ni alloy electrodeposition from acid sulphate bath, J. Appl. Electrochem., v. 41, (2011) 535–541

[25] J.R. Garcia; D.C. Baptista do Lago; L. Ferreira de Senna: Materials research, Electrodeposition of Cobalt Rich Zn-Co alloy Coatings from citrate bath, v.17, No. 4, (2014) 947–957

[26] K.O. Nayana; T.V. Venkatesha; B.M. Praveen; K. Vathsala: Synergistic effect of additives on bright nanocrystalline Zn electrodeposition, J. Appl. Electrochem., v. 41, (2011) 39–49

[27] A.K.N. Reddy: Preferred orientation in nickel electrodeposits: The mechanism of development of textures in nickel electrodeposits, J. Electro analytical Chem., v. 6, No. 2, (1963) 141–152

Authors

Prof. Dr. S. Basavanna
Department of Chemistry, Prerana PU College, Tumkur-572103, Karnataka, INDIA
Email: drsbasavanna@gmail.com
Phone: +91 9901984626

Ass. Prof. Jyoti Shankarrao Kavirajwar
Department of Chemistry, APS College of Arts and Science, Bangalore, Karnataka, INDIA
Email: jyotimaheshramojwar@gmail.com

CONTACT:

EUGEN G. LEUZE VERLAG KG
Ralf Schattmaier
Karlstraße 4
88348 Bad Saulgau
Germany

Email: ralf.schattmaier@leuze-verlag.de
Phone: +49 (0) 7581 4801-12
Fax: +49 (0) 7581 4801-10